BJR

BONE BIOLOGY

Platelet-derived extracellular vesicles promote osteoinduction of mesenchymal stromal cells

M. Antich-Rosselló,
M. A. Forteza-Genestra,
J. Calvo,
A. Gayà,
M. Monjo,
J. M. Ramis

From Institut d'Investigació Sanitària de les Illes Balears (IdISBa), Palma de Mallorca, Spain

Aims

Platelet concentrates, like platelet-rich plasma (PRP) and platelet lysate (PL), are widely used in regenerative medicine, especially in bone regeneration. However, the lack of standard procedures and controls leads to high variability in the obtained results, limiting their regular clinical use. Here, we propose the use of platelet-derived extracellular vesicles (EVs) as an off-the-shelf alternative for PRP and PL for bone regeneration. In this article, we evaluate the effect of PL-derived EVs on the biocompatibility and differentiation of mesenchymal stromal cells (MSCs).

Methods

EVs were obtained first by ultracentrifugation (UC) and then by size exclusion chromatography (SEC) from non-activated PL. EVs were characterized by transmission electron microscopy, nanoparticle tracking analysis, and the expression of CD9 and CD63 markers by western blot. The effect of the obtained EVs on osteoinduction was evaluated in vitro on human umbilical cord MSCs by messenger RNA (mRNA) expression analysis of bone markers, alkaline phosphatase activity (ALP), and calcium (Ca^{2+}) content.

Results

Osteogenic differentiation of MSCs was confirmed when treated with UC-isolated EVs. In order to disprove that the effect was due to co-isolated proteins, EVs were isolated by SEC. Purer EVs were obtained and proved to maintain the differentiation effect on MSCs and showed a dose-dependent response.

Conclusion

PL-derived EVs present an osteogenic capability comparable to PL treatments, emerging as an alternative able to overcome PL and PRP limitations.

Cite this article: *Bone Joint Res* 2020;9(10):667–674.

Keywords: Extracellular vesicles, Mesenchymal stromal cells, Platelet lysate.

Article focus

- Use of platelet-derived extracellular vesicles (EVs) for bone regenerative applications.
- In vitro evaluation of the biocompatibility and bioactivity of platelet-derived EVs.

Key messages

- Platelet-derived EVs induce the differentiation towards the osteogenic lineage of mesenchymal stromal cells (MSCs).
- Platelet-derived EVs could be used as a reproducible, standardized, and off-the-shelf allogeneic treatment.

Strengths and limitations

- Here we demonstrate the osteogenic capacity of platelet-derived EVs to be used for bone regenerative applications. Our alternative would overcome the drawbacks of platelet concentrates, since it would provide an off-the-shelf controlled product.
- One limitation of the study could be the use of small EVs obtained from non-stimulated platelets; there exists the possibility that we have missed EV preparations with higher effects than the ones used in the study.

Correspondence should be sent to Joana M Ramis; email: joana.ramis@uib.es

doi: 10.1302/2046-3758.910.BJR-2020-0111.R2

Bone Joint Res 2020;9(10):667–674.

- The results obtained in the present study should now be validated in a proof-of-concept animal study.

Introduction

Platelet-rich plasma (PRP) and platelet lysate (PL) are platelet concentrates widely used in bone regeneration.[1–3] Despite the promising regenerative results of PL and PRP, their use has not yet been established as normal procedure. On the one hand, autologous concentrates are normally used, and the volume obtained can be limited;[2] some patients are not even suited for these interventions due to their medical history.[4] On the other hand, the lack of reproducibility - mainly due to non-standardized separation methods, donor variability, storage conditions,[5-8] or the use of external activators like thrombin or calcium (Ca^{2+})- hinder subsequent clinical use.[9]

Previous studies have shown that PL induces mesenchymal stromal cell (MSC) differentiation towards the osteogenic lineage.[10,11] MSC differentiation may be due to different biomolecules,[12,13] but a recent study points out that more complex systems like extracellular vesicles (EVs) may also be involved.[14] When discussing PL or PRP, the growth factors contained in platelets were thought to be the main messengers in the wound healing processes.[15–17] Nevertheless, recent research has revealed that active RNAs and EVs, formerly reported as 'platelet dust',[18] also have an important role in platelet-cell communication[19] and, in turn, in its regenerative effects. The use of EVs instead of platelet concentrates would allow their off-the-shelf allogeneic use.

Platelets have been shown to produce a heterogeneous population of EVs, with most of them having sizes between 100 nm and 250 nm.[20] These EVs have been isolated through different techniques, which include ultracentrifugation (UC), size exclusion chromatography (SEC), or antibody-covered beads.[20] Platelet-derived EVs present specific protein markers like tetraspanins[21] and contain different active biomolecules like RNAs[22] and growth factors.[10] Nevertheless, platelet-derived EVs are highly diverse and their characteristics depend on the external factors that the platelets have been exposed to during EV production and release.[23] Few studies have explored the use of platelet-derived EV in tissue regeneration in vitro[10] and in vivo,[24,25] focusing on the contribution of EVs to PL activity.

Here, we aimed to evaluate whether EVs preserve the effects of platelet concentrates on MSC differentiation in order to propose an off-the-shelf product that could maintain the regenerative effects while overcoming the main drawbacks of using platelet concentrates. Furthermore, EVs could be formulated for treatment as different pharmaceutical forms or combined with biomaterials.[26–29]

Methods

Human PL preparation. Fresh buffy coats, containing 25% to 40% of residual plasma, were obtained from the IdISBa Biobank. The inclusion and exclusion criteria for blood donation were met, excluding donors who had taken non-steroidal anti-inflammatories. Briefly, six buffy coats were washed with 0.9% NaCl and pooled, obtaining a platelet concentrate after a centrifugation and leucocyte filtration. The platelet concentration was adjusted at 1,200 × 10^9 to 1,800 × 10^9 platelets/l, followed by three freeze/thawing cycles (-80°C/37°C) to lysate more than 80% of platelets. Centrifuged for 20 minutes at 3,900 rpm, the supernatant was filtered by 0.4 µm pore size membrane (Sartorius, Goettingen, Germany) and further centrifuged for 15 minutes at 1,500 ×g at 4°C. The supernatant was then filtered (0.8 µm) before being used for treatment or for EV isolation by UC or SEC (Supplementary Figure aa).

Isolation of PL-EVs by UC. PL was diluted (1/20) in PBS (Biowest, Nuaillé, France), filtered (0.2 µm), and centrifuged at 10,000 ×g for 30 minutes at 4°C to eliminate large- and medium-sized vesicles and supernatant was centrifuged at 120,000 ×g for 18 hours at 4°C (Ultracentrifuge Optima-L-100XP, SW32-Ti-rotor; Beckman Coulter, Brea, California, USA). The pellet was resuspended in 300 µl of PBS. UC-EVs were stored at -80°C until use.

Isolation of PL-EVs by SEC. PL was directly filtered (0.2 µm) and then centrifuged at 10,000 ×g for 30 minutes at 4°C to eliminate large- and medium-sized vesicles. The supernatant (1.5 ml) was loaded on a hand-made SEC column (Sepharose-CL-2B; Sigma-Aldrich, St. Louis, Missouri, USA) and was stacked into a 10 ml syringe (BD Biosciences, Franklin Lakes, New Jersey, USA), stuffed with nylon stocking (Calzedonia, Dossobuono, Italy), and washed with 10 ml phosphate-buffered saline (PBS). In all, 24 fractions of 0.5 ml were eluted; total protein concentration and presence of specific markers were performed for each fraction. Fractions 6 to 12, enriched in EVs, were pooled and characterized.

Transmission electron microscopy. EV samples were fixed in 2% formaldehyde (Sigma-Aldrich) and set on copper Formvar-Carbon-coated grids (Ted Pella, Redding, California, USA) for 20 minutes. After washing the grids with PBS, samples were incubated with 1% glutaraldehyde (Sigma-Aldrich) for five minutes and washed with deionized water. The samples were stained for one minute with 2% phosphotungstic acid and air-dried. Images were taken using a transmission electron microscope (TEM)-H600 (Hitachi, Tokyo, Japan) at 50 kV.

Nanoparticle tracking analysis. The number of particles and size were measured with a ZetaView Nanoparticle-Tracking-Analyzer (ParticleMetrix-GmbH, Meerbush, Germany). Samples were diluted (1/1,000) before analyzing 22 positions' tracks per video.

Protein quantification. Total protein was quantified either with the BCA Protein Assay Kit (Thermo Fisher, Waltham, Massachusetts, USA) or with a Nanodrop2000 (Thermo Fisher) at λ = 280 nm.

Western blot. PL and EV samples were prepared with non-reducing Laemli loading buffer[30] and denatured at 70°C for ten minutes. Samples were loaded in a 10% to 12% gradient sodium dodecyl sulphate-polyacrylamide gel electrophoresis (SDS-PAGE) gel and proteins were separated by electrophoresis. The transfer was performed onto nitrocellulose membrane (GE Healthcare, Pittsburgh, Pennsylvania, USA)

Table I. Genes and primers used for gene expression analysis. "S" stands for sense primers and "A" stands for antisense primers.

Gene	Primer sequence (5'→ 3')	Product size, bp	GeneBank accession number
COL1A1	S: CCTGACGCACGGCCAAGAGG A: GGCAGGGCTCGGGTTTCCAC	122	NM_000088.4
SPP1	S: ATCTCCTAGCCCCACAGACC A: TCCGTGGGAAAATCAGTGACC	217	NM_000582.2
SP7	S: AGGTTCCCCCAGCTCTCTCCATCTG A: AATTTGCTGCACGCTGCCGTC	139	NM_001173467.3
RUNX2	S: CTGTGCTCGGTGCTGCCCTC A: CGTTACCCGCCATGACAGTA	118	NM_004348
SOX9	S: GCTCTGGAGACTTCTGAACGA A: CCGTTCTTCACCGACTTCCT	132	NM_000346.3
Rn18s	S: GTAACCCGTTGAACCCCATT A: CCATCCAATCGGTAGTAGCG	151	NR_003278.3
GAPDH	S: TGCACCACCAACTGCTTAGC A: GGCATGGACTGTGGTCATGAG	87	M33197
B2M	S: CACTGAATTCACCCCCACTGA A: GCGGCATCTTCAAACCTCCA	129	NM_004048.3
ACTB	S: CTGGAACGGTGAAGGTGACA A: AAGGGACTTCCTGTAACAA	140	NM_001101.5

ACTB, Actin β; B2M, Beta-2-microglobulin; bp, base pair; COL1A1, Collagen type I α 1 chain; GAPDH, Glyceraldehyde-3-phosphate dehydrogenase; Rn18s, 18s ribosomal RNA ; RUNX2, Runt-related transcription factor 2; SOX9, Sapiens SRY-box 9; SP7, Osterix; SPP1, Osteopontin.

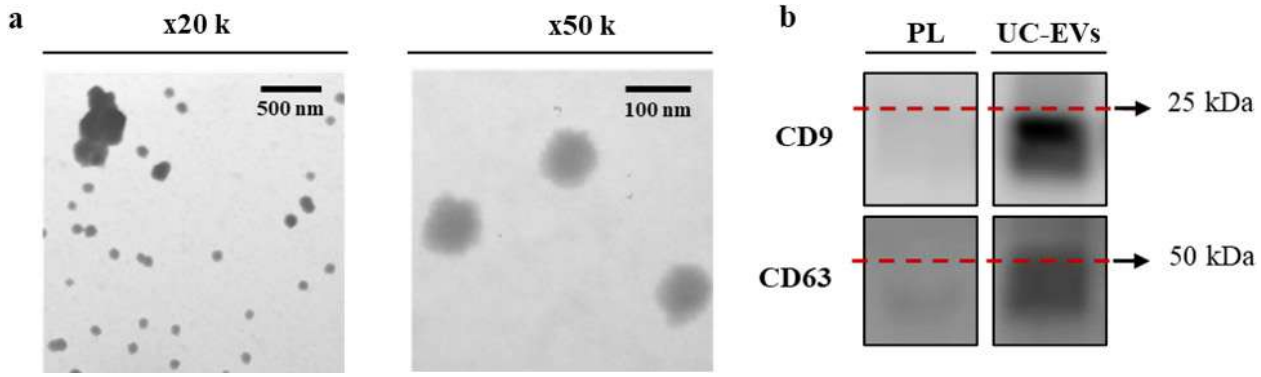

Fig. 1

a) Morphological characterization of ultracentrifuged extracellular vesicles (UC-EVs) by transmission electron microscopy imaging. Images were taken at ×20,000 augments (wide-field) and at ×50,000 augments (close-up). b) Presence of EV biomarkers CD9 and CD63 for PL and the UC-EVs determined by western blot. The same amount of protein was loaded per well (5 µg).

with humid conditions. A five-minute incubation with 0.2% (w/v) Ponceau-S (Sigma-Aldrich) and 3% (v/v) acetic acid solution (Sigma-Aldrich) was performed for total protein visualization.

Membranes were incubated for one hour with blocking buffer with 10% dry skimmed milk (Central Lechera Asturiana, Granda, Spain). Primary antibody incubation was performed overnight with 1/2,000 dilutions of the following antibodies: anti-human CD9 (Thermo Fisher) and anti-human CD63 (Abcam, Cambridge, UK). Secondary antibody one-hour incubation was performed with 1/2,000 diluted horseradish peroxidase (HRP)-coupled anti-mouse immunogloblin G (IgG) (Thermo Fisher). Chemiluminescence detection with Clarity Western ECL Substrate (Bio-Rad, Hercules, California, USA), C-DiGit Blot scanner, and Image Studio-Digits Software 4.0 (LI-COR Biosciences, Lincoln, Nebraska, USA) were used for membrane exposure and image processing.

Cell culture. Human umbilical cord MSCs were obtained from the IdISBa Biobank. Their use was approved by its Ethics Committee (IB1955/12BIO). MSCs were cultured at 37°C and 5% CO_2, using Dulbecco's Modified Eagle Medium (DMEM)–low glucose (Biowest) with 100 µg/ml penicillin-streptomycin (Biowest) and 20% foetal bovine serum (FBS) embryonic stem cells tested (Biowest). Half of the medium was changed every three days.

For treatment, 30,000 cells/cm^2 were seeded, at confluence, two PBS washes were performed and treated: Control (PBS), PL (2.6 µg/cm^2 of PL), UC-EVs (2.6 µg/cm^2 of UC isolated EVs, equivalent to 3.5 × 10^6 part/cm^2), low dose (LD)-SEC-EVs (3.5 × 10^6 part/cm^2 of SEC isolated EVs), and high dose (HD)-SEC-EVs (3.0 × 10^{10} part/cm^2 of SEC isolated EVs). The treatment of UC-EVs was normalized by the amount of proteins used in the PL group, which was set in preliminary studies (data not shown). For LD-SEC-EVs, the same amount

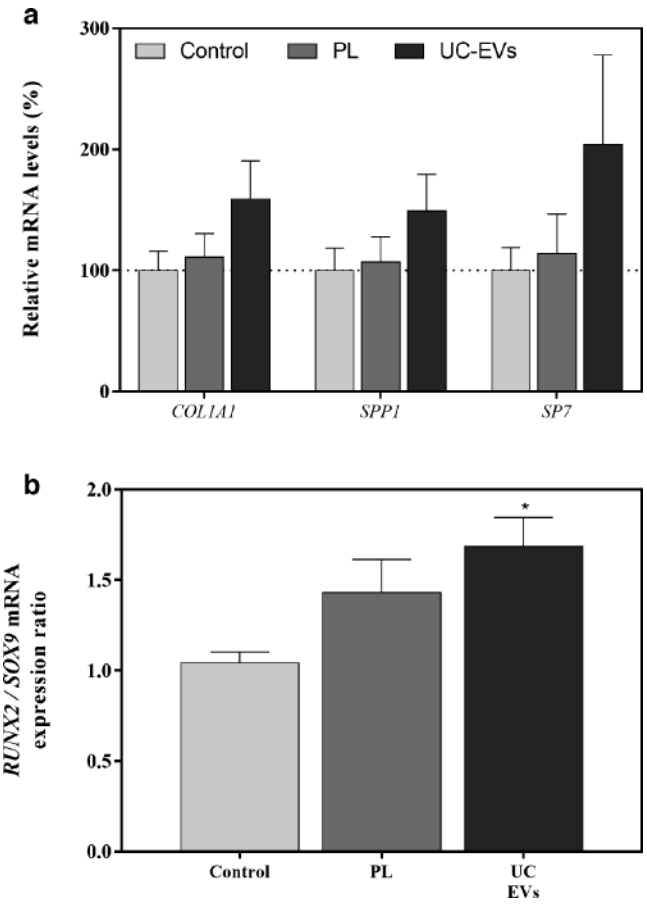

Fig. 2

a) Messenger RNA (mRNA) expression levels in mesenchymal stromal cells (MSCs) after 14 days of platelet lysate (PL) and ultracentrifuged extracellular vesicle (UC-EV) treatments of collagen type I α 1 chain (COL1A1), Osteopontin (SPP1), and Osterix (SP7). Data represent the mean and standarderror of the mean (SEM) for each group. Gene expression levels were normalized to reference genes and to the control group, which was set to 100%. b) Runt-related transcription factor 2 (RUNX2)/Sapiens SRY-box 9 (SOX9) ratio mRNA levels were divided by the SOX9 mRNA levels. Data represent the mean and SEM for each group. Results were compared using the Kruskal-Wallis test. *Statistically significant ($p < 0.05$) differences compared to the control group.

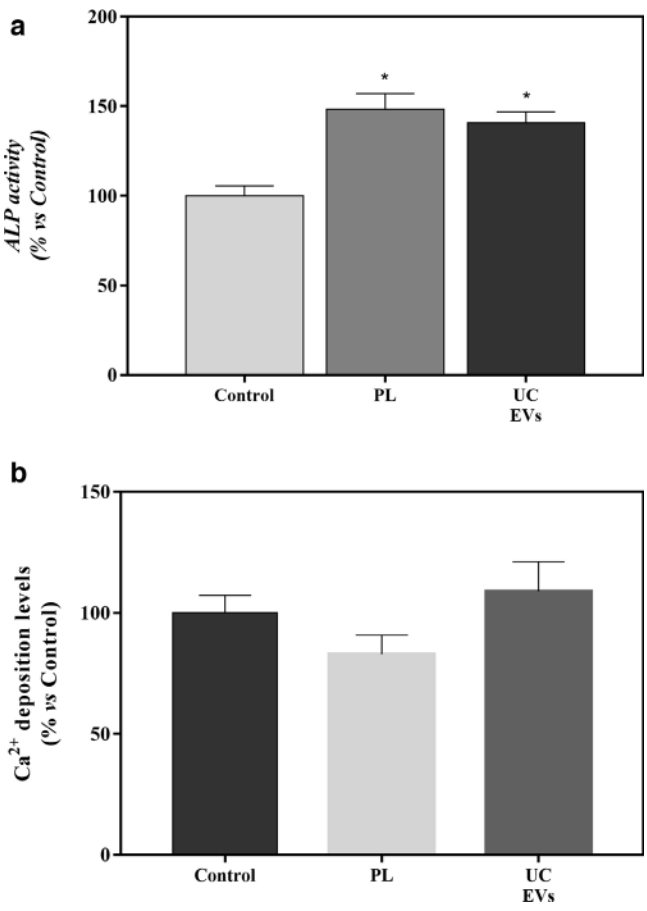

Fig. 3

a) Alkaline phosphatase (ALP) activity from cellular lysate of mesenchymal stromal cells (MSCs) after 14 days of platelet lysate (PL) and ultracentrifuged extracellular vesicle (UC-EV) treatments. Data were normalized to the control group, set to 100%. Data were compared using Kruskal-Wallis test. *Statistically significant differences ($p < 0.05$) compared to the control group. b) Calcium (Ca^{2+}) deposition on the cell monolayer after 14 days of PL and UC-EV treatments. Data represent the mean and SEM for each group. Data were normalized to the control group, set to 100%. Data were compared using analysis of variance (ANOVA) and Bonferroni as post hoc.

of particles as UC-EVs was used. Finally, a 50-fold amount of proteins versus PL was used for the HD-SEC-EV treatment.

Treatments were given in DMEM Low Glucose (Biowest), 100 µg/ml penicillin-streptomycin, and 1% FBS-EVs depleted by centrifugation at 120,000 xg for 18 hours at 4°C. Medium and treatments were refreshed every three days.

Alkaline phosphatase activity. Cellular alkaline phosphatase (ALP) activity was measured at 14 days. Cells were lysed with 0.1% Triton X-100 in PBS performing two freeze/thaw cycles. ALP activity was evaluated with p-Nitrophenyl Phosphate (Sigma-Aldrich).

Calcium content determination. Lysed cells from the ALP activity assay were diluted 1:1 in 1 N HCl and total Ca^{2+} content was evaluated by inductively coupled plasma atomic emission spectrometry (Optima 5300 DV; PerkinElmer, Waltham, Massachusetts, USA). Data were compared with the $CaCl_2$ standard curve included in the assay.

RNA isolation and real-time RT-PCR. Total RNA was isolated using RNAzol RT (Molecular Research Center, Cincinnati, Ohio, USA), according to the manufacturer's protocol. The same amount of RNA was loaded for reverse transcription using High Capacity RNA-to-cDNA Kit (Applied Biosystems, Foster City, California, USA).

Real-time polymerase chain reaction (RT-PCR) was performed using the Lightcycler480 thermocycler (Roche Diagnostics, Basel, Switzerland) following the manufacturer's instructions using specific primers (Table I). Crossing points were used to calculate the expression of each. Reference genes were used to normalize the target genes' expression levels and changes were compared to the control group, set to 100%.

Statistical analysis. For statistical analysis, SPSS v.25.0 (IBM, Armonk, New York, USA) was used. Normality was

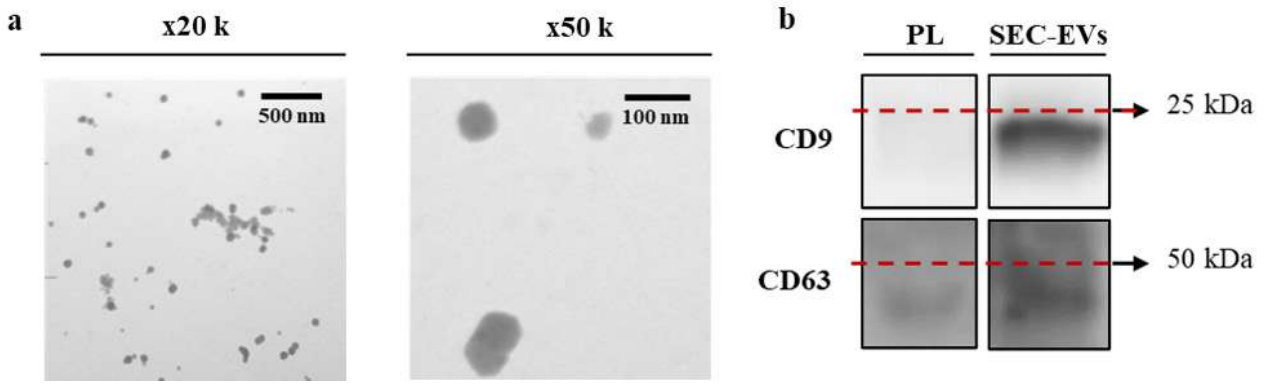

Fig. 4

a) Morphological characterization of size exclusion chromatography extracellular vesicles (SEC-EVs) by transmission electron microscopic imaging. Images were taken at ×20,000 augments (wide-field) and ×50,000 augments (close-up). b) Presence of EV biomarkers CD9 and CD63 for platelet lysate (PL) and the SEC-EVs determined by western blot. The same amount of protein was loaded per well (5 µg).

determined using Shapiro-Wilk test. Kruskal-Wallis test or one-way analysis of variance (ANOVA) (Bonferroni or Games-Howell as post-hoc) were performed. Results were considered statistically significant at $p < 0.05$.

Results

UC-EV characterization. International Society for Extracellular Vesicles (ISEV) recommendations were followed for EV isolation and characterization.[31] Electron microscopy was used to confirm the presence of vesicles (Figure 1a). TEM wide-field images from UC-EVs showed a highly homogeneous population of vesicles with the presence of some small aggregates. Close-up images from UC-EVs showed an average size around 100 nm. The presence of the EV markers CD9 and CD63 was also confirmed (Figure 1b). Particles were also analyzed by nanoparticle tracking analysis (NTA) (Supplementary Figure ab), showing a particle content of 2.9×10^{10} particles/ml and a mean size of 217 nm (SD 8). In terms of purity,[32] a ratio of 1.7×10^{6} particles/µg of protein was obtained.

UC-EV functional study. To evaluate the effects of the PL-derived EVs, an in vitro functional study was performed using MSCs (Supplementary Figure ac). COL1A1, SP7, and SPP1 messenger RNA (mRNA) expression levels were higher for the PL and UC-EV treated groups after 14 days of treatment (Figure 2a), despite not reaching statistical significance. RUNX2/SOX9 mRNA ratio was significantly higher in cells treated with UC-EVs compared to the control group, while no significance was reached in cells treated with PL despite being higher than the control group (Figure 2b).

Moreover, ALP activity, a marker of osteoblast differentiation, and Ca^{2+} deposition on the cell monolayer were determined (Figure 3a and 3b). PL and UC-EV treated groups presented higher ALP activity than the control group. However, there were no differences in Ca^{2+} deposition.

SEC-EV characterization. To obtain purer EV samples, we used SEC since it allows a higher separation from proteins.[33] Total protein amount and presence of CD9 was evaluated on the obtained SEC fractions (Supplementary Figures ad and ae). Fractions enriched in EVs (6 to 12) were selected, pooled, and used for treatment.

The presence of vesicles in SEC-EV samples was confirmed by TEM and WB (Figure 4). Wide-field images and close-up images (Figure 4a) from SEC-EVs showed vesicles around 100 nm with the presence of some aggregates. The EV markers CD9 and CD63 were also present in the SEC-EV samples (Figure 4b). Particle analysis by NTA (Supplementary Figure ab) revealed a particle content of 4.8×10^{10} particles/ml. The mean size for SEC-EVs was 197 nm (SD 3), statistically different compared by independent-samples *t*-test ($p = 0.001$) from that observed for UC-EVs (217 nm (SD 8)). Moreover, higher purity was obtained for SEC-EVs (2.0×10^{8} particles/µg) compared to UC-EVs (1.7×10^{6} particles/µg).

SEC-EV functional study. Both SEC-EV-treated groups presented higher ALP activity than the control group, showing that the higher dose had higher values than the lower dose (Figure 5a). Ca^{2+} content was higher in the treated groups, although statistical significance was only found for the high dose: HD-SEC-EV group (Figure 5b).

Discussion

PRP and PL have already been described as showing bone regenerative effects.[10,11,16,34] However, the complexity of the samples, their variability depending on their source, production method, and storage conditions have hindered their clinical use.[35] Here we demonstrate that EVs derived from platelet concentrates preserve and even increase their osteogenic effects. For this reason, we propose their use as an alternative treatment to overcome PL and PRP limitations.

Here, we demonstrate that both PL and PL-derived EVs promote MSC differentiation towards the osteogenic lineage. On the one hand, we have investigated osteoinductivity through the analysis of the expression of different osteoblast markers in the absence of osteogenic supplements. *RUNX2* is the master gene necessary for the osteoblast lineage commitment. However, it has been proposed

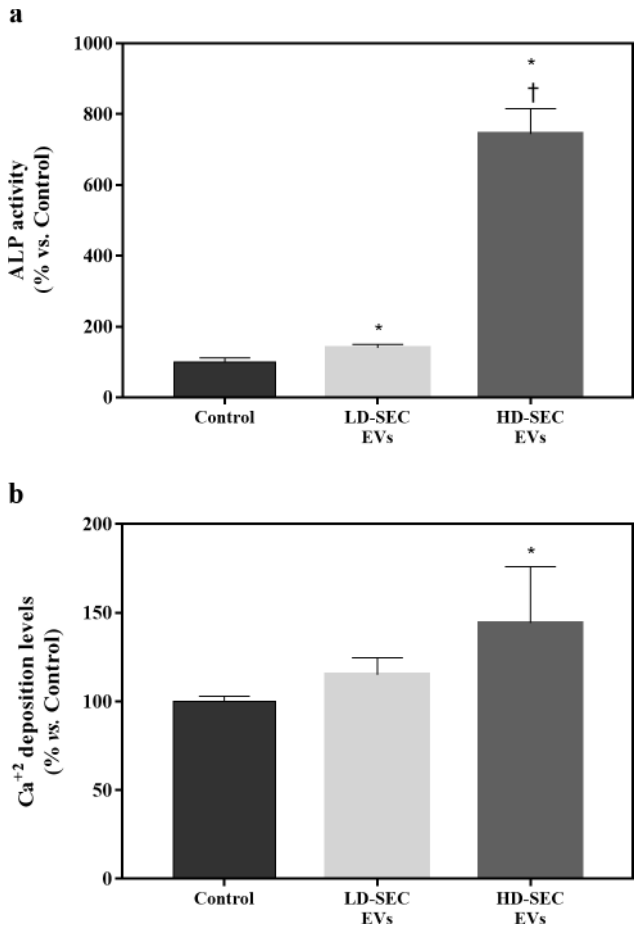

Fig. 5

a) Alkaline phosphatase (ALP) activity from cellular lysate after 14 days of low dose size exclusion chromatography extracellular vesicle (LD-SEC-EV) and high dose (HD)-SEC-EV treatments. Data were normalized to the control group, set to 100%. Results were compared using analysis of variance (ANOVA) and Games-Howells as post hoc. b) Calcium (Ca^{2+}) deposition on the cell monolayer after 14 days of LD-SEC-EV and HD-SEC-EV treatments. Data represent the mean and SEM for each group. Data were normalized to the control group, set to 100%. Results were compared using ANOVA and Games-Howells as post hoc. *Statistically significant ($p < 0.05$) differences compared to the control group. †Statistically significant differences compared to LD-SEC-EVs.

that the *RUNX2/SOX9* ratio is the most indicative predictor for osteogenicity of human MSCs.[36] Here we report a significantly increased ratio in MSC cells treated with UC-EVs, and a tendency towards increased mRNA expression levels of other osteoblast markers such as *SP7*, *SPP1*, and *COL1A1*. During osteogenic differentiation, *RUNX2* activates the expression of Osterix, a specific osteogenic transcription factor involved in the differentiation step from preosteoblast to fully functional osteoblast.[37] While type I collagen is highly expressed in the early synthetic stage supporting cell proliferation,[38] Osteopontin, a sialoprotein that mediates hydroxyapatite binding, shows high expression levels after mineralization has been initiated.[39]

On the other hand, in agreement with the gene expression results, significantly higher ALP activity was confirmed for MSCs treated with UC-EVs compared to the control group. ALP contributes to the generation of an extracellular matrix competent for mineralization, and it is the most widely recognized biochemical marker for osteoblast activity.[38] Thus, our results point to an osteogenic induction of MSCs by platelet-derived EVs.

Since the effect of platelet concentrates is usually explained by its content on growth factors, and protein contamination has been shown in pellets of EVs obtained by UC,[32] we raised the possibility that our results could be undervalued due to proteins co-isolated with EVs and not due to the EVs themselves. To discard this possibility, we used size exclusion chromatography to separate EV fractions from proteins.[33] We started using UC because this was the gold standard protocol, but indeed, SEC-EV samples presented higher purity by up to two orders of magnitude than the UC-EV ones. Nevertheless, both of them are below 1.5×10^9 particles/µg, established as unpure by Webber and Clayton.[32] However, this classification was established for cell culture media or urine-derived vesicles, both sources containing lower protein content than PL. Thus, new border categories should be established according to the complexity of the EV's source. In any case, we show that SEC purification increased purity 115-fold compared to UC.

Some authors suggest that the isolation methodology used may alter the EV population obtained as well as change its functionality.[40,41] In our case, SEC-EVs were smaller than UC-EVs according to the NTA results. Other studies have reported the same phenomenon; it has been attributed to aggregation or fusion between EVs during UC isolation induced by the high speed and an enrichment with larger EVs, due to their increased ability to sediment when being centrifuged compared to the small ones.[41] Moreover, our results confirm that PL-EV TEM sizes are smaller than those obtained by NTA, in agreement with Aatonen et al.[20] TEM size results are not as reliable as NTA results, due to the dehydrating fixing steps prior to TEM visualization and the lower statistical power of TEM compared to NTA.[31] According to the ISEV nomenclature,[31] small EVs CD9+ and CD63+ are enriched in both samples. Another notorious difference between isolation methods is the aforementioned purity of the obtained EVs. Overall, although UC is considered the gold standard for EV isolation, it is worth comparing the effects from other isolation techniques, especially when EVs must be used in therapeutics[41,42] since UC is believed to alter the nature of EVs by applying high shear forces during high-speed UC.[43] Our results confirmed the osteogenic effect of platelet-derived EVs on MSCs; we observed increased ALP activity in cells treated with SEC-EVs, supporting EVs as osteoinductive effectors. Furthermore, a dose-dependent effect is suggested by the higher ALP activity and Ca^{2+} deposition induced by the HD-SEC-EVs. A direct comparison between UC-EVs, SEC-EVs, and PL (Supplementary Figure af) shows that both isolation methods induce similar osteogenic effects, comparable to those induced by the PL (the latter containing exosomes in a

lower concentration than EV isolates, plus growth factors released from platelets).

Small platelet-derived EVs have been pointed out as possible active PL effectors for bone healing applications, though osteogenic supplements (dexametasone, β-glycerol phosphate, and ascorbic acid) were added to cell culture media in those previous experiments.[10] Here, we demonstrate the intrinsic osteoinductive effect of small platelet-derived EVs, showing induction of MSC differentiation towards the osteogenic lineage without adding any external inducer. Even more, we evaluated not only UC but also SEC, demonstrating that platelet-derived EVs can be an effective substitute for platelet concentrates in regenerative medicine.

It is worth mentioning that some studies have previously shown that PL could be a potential substitute for FBS in the propagation and maintenance of undifferentiated MSCs.[44] However, our results suggest that PL without any osteogenic supplement is capable of inducing bone differentiation. This fact would hinder the ability to maintain MSCs without modifying their differentiation capabilities. Nevertheless, dose could have an important role in the effects described. In this study, low PL doses have been used (2.6 μg of total protein/cm^2, namely 0.02 ml of PL per 100 ml in the cell culture media in combination with a 1% EV-depleted FBS) while 10% of PL is normally used in substitution of FBS for MSC maintenance.[45] Further studies should be performed to evaluate the dose-effect response of PL and affirm the potential to use it as a FBS xeno-free substitute.

With regards to platelet concentrates on bone regeneration, despite promising results[1–3] their use in clinics entails some drawbacks: there is the lack of standardized protocols and quality controls,[1,4] but there is also variability among patients, leading to high heterogeneity of the obtained concentrates.[2,5] Alternatively, we propose the use of EVs obtained from pools of human-certified buffy coats otherwise discarded after fractionation of donated blood. Here, we confirmed the previous observations of PL activity on bone regeneration, confirming its content in important and potent activating factors. Among these factors, our results suggest EVs are significant effectors of PL activity on bone differentiation, as shown by the higher osteoinductive dose-dependent effect that we found when using highly purified EVs, thus presenting a better opportunity than PL or PRP for future in vivo and clinical experiments. Our enhanced results obtained with EVs versus PL could be explained by a protective encapsulation of active biomolecules offered by the vesicles themselves.[46]

Our study entails some limitations: firstly, the lack of physiological platelet microvesiculation induction by stimulation with agonists or by platelet storage before EV isolation; secondly, the selection of small EVs (formerly referred as exosomes) instead of using both small- and medium-sized EVs. The possibility of obtaining EV preparations with even higher effects should be further explored.

However, considering the osteogenicity we showed, PL-derived EVs could be used as a reproducible, standardized, and off-the-shelf allogeneic treatment. Moreover, PL-derived EVs may also take different pharmaceutical forms or be combined with biomaterials such as polymeric scaffolds, tricalcium phosphate, or collagen membranes, which are already under study with cell line-derived EVs.[26–29]

In conclusion, PL-derived EVs are important effectors for MSC osteogenic differentiation in a dose-dependent manner. Therefore, we propose their use in bone regenerative medicine as an alternative to overcome PL and PRP limitations.

Supplementary material

A schematic description of EV isolation methods, the NTA characterization histogram of EVs, the characterization of the isolated fractions obtained by SEC, and a functional comparison between UC-isolated EVs and SEC-isolated EVs.

References

1. **Zamani M**, **Yaghoubi Y**, **Movassaghpour A**, **et al**. Novel therapeutic approaches in utilizing platelet lysate in regenerative medicine: are we ready for clinical use? *J Cell Physiol*. 2019;234(10):17172–17186.
2. **Marques LF**, **Stessuk T**, **Camargo ICC**, **et al**. Platelet-rich plasma (PRP): methodological aspects and clinical applications. *Platelets*. 2015;26(2):101–113.
3. **Cancedda R**, **Bollini S**, **Descalzi F**, **Mastrogiacomo M**, **Tasso R**. Learning from mother nature: innovative tools to boost endogenous repair of critical or difficult-to-heal large tissue defects. *Front Bioeng Biotechnol*. 2017;5:28.
4. **The International Cellular Medical Society**. 206_ICMS - Guidelines for the use of Platelet Rich Plasma - Draft. 2010. http://www.apexbiologix.com/wp-content/uploads/2014/06/PRP-Guidelines-Technique-and-Protocols-by-The-International-Cellular-Medical-Society.pdf (date last accessed 1 October 2020).
5. **Lippross S**, **Alini M**. Platelet-rich plasma for bone healing—to use or not to use? *AO Dialogue*. 2007:25–29.
6. **Fadadu PP**, **Mazzola AJ**, **Hunter CW**, **Davis TT**. Review of concentration yields in commercially available platelet-rich plasma (PRP) systems: a call for PRP standardization. *Reg Anesth Pain Med*. 2019:652–659.
7. **Rossi LA**, **Murray IR**, **Chu CR**, **et al**. Classification systems for platelet-rich plasma. *Bone Joint J*. 2019;101-B(8):891–896.
8. **Berger DR**, **Centeno CJ**, **Steinmetz NJ**. Platelet lysates from aged donors promote human tenocyte proliferation and migration in a concentration-dependent manner. *Bone Joint Res*. 2019;8(1):32–40.
9. **Ahmed M**, **Reffat SA**, **Hassan A**, **Eskander F**. Platelet-Rich plasma for the treatment of clean diabetic foot ulcers. *Ann Vasc Surg*. 2017;38:206–211.
10. **Torreggiani E**, **Perut F**, **Roncuzzi L**, **et al**. Exosomes: novel effectors of human platelet lysate activity. *Eur Cell Mater*. 2014;28:137–151. discussion 151.
11. **Jonsdottir-Buch SM**, **Lieder R**, **Sigurjonsson OE**. Platelet lysates produced from expired platelet concentrates support growth and osteogenic differentiation of mesenchymal stem cells. *PLoS One*. 2013;8(7):e68984.
12. **Wu T**, **Zhang J**, **Wang B**, **et al**. Staphylococcal enterotoxin C2 promotes osteogenesis of mesenchymal stem cells and accelerates fracture healing. *Bone Joint Res*. 2018;7(2):179–186.
13. **Xie X**, **Liu M**, **Meng Q**. Angelica polysaccharide promotes proliferation and osteoblast differentiation of mesenchymal stem cells by regulation of long non-coding RNA H19: an animal study. *Bone Joint Res*. 2019;8(7):323–332.
14. **Ferreira E**, **Porter RM**. Harnessing extracellular vesicles to direct endochondral repair of large bone defects. *Bone Joint Res*. 2018;7(4):263–273.
15. **Pietramaggiori G**, **Kaipainen A**, **Czeczuga JM**, **Wagner CT**, **Orgill DP**. Freeze-dried platelet-rich plasma shows beneficial healing properties in chronic wounds. *Wound Repair Regen*. 2006;14(5):573–580.
16. **Kim J**, **Ha Y**, **Kang NH**. Effects of growth factors from platelet-rich fibrin on the bone regeneration. *J Craniofac Surg*. 2017;28(4):860–865.

17. **Schär MO**, **Diaz-Romero J**, **Kohl S**, **Zumstein MA**, **Nesic D**. Platelet-rich concentrates differentially release growth factors and induce cell migration in vitro. *Clin Orthop Relat Res*. 2015;473(5):1635–1643.
18. **van der Pol E**, **Harrison P**. From platelet dust to gold dust: physiological importance and detection of platelet microvesicles. *Platelets*. 2017;28(3):211–213.
19. **Preußer C**, **Hung L-H**, **Schneider T**, **et al**. Selective release of circRNAs in platelet-derived extracellular vesicles. *J Extracell Vesicles*. 2018;7(1):1424473.
20. **Aatonen MT**, **Öhman T**, **Nyman TA**, **et al**. Isolation and characterization of platelet-derived extracellular vesicles. *J Extracell Vesicles*. 2014;3(1):24692.
21. **Heijnen HF**, **Schiel AE**, **Fijnheer R**, **Geuze HJ**, **Sixma JJ**. Activated platelets release two types of membrane vesicles: microvesicles by surface shedding and exosomes derived from exocytosis of multivesicular bodies and alpha-granules. *Blood*. 1999;94(11):3791–3799.
22. **Santoso S**, **Moebus A**, **Schreiner S**, **et al**. Selective release of circRNAs in platelet-derived extracellular vesicles. *J Extracell Vesicles*. 2018;7(1):1424473.
23. **Ponomareva AA**, **Nevzorova TA**, **Mordakhanova ER**, **et al**. Intracellular origin and ultrastructure of platelet-derived microparticles. *J Thromb Haemost*. 2017;15(8):1655–1667.
24. **Xu N**, **Wang L**, **Guan J**, **et al**. Wound healing effects of a Curcuma zedoaria polysaccharide with platelet-rich plasma exosomes assembled on chitosan/silk hydrogel sponge in a diabetic rat model. *Int J Biol Macromol*. 2018;117:102–107.
25. **Guo S-C**, **Tao S-C**, **Yin W-J**, **et al**. Exosomes derived from platelet-rich plasma promote the re-epithelization of chronic cutaneous wounds via activation of YAP in a diabetic rat model. *Theranostics*. 2017;7(1):81–96.
26. **Qi X**, **Zhang J**, **Yuan H**, **et al**. Exosomes secreted by human-induced pluripotent stem cell-derived mesenchymal stem cells repair critical-sized bone defects through enhanced angiogenesis and osteogenesis in osteoporotic rats. *Int J Biol Sci*. 2016;12(7):836–849.
27. **Zhang J**, **Liu X**, **Li H**, **et al**. Exosomes/tricalcium phosphate combination scaffolds can enhance bone regeneration by activating the PI3K/Akt signaling pathway. *Stem Cell Res Ther*. 2016;7(1):136.
28. **Li W**, **Liu Y**, **Zhang P**, **et al**. Tissue-Engineered bone immobilized with human adipose stem cells-derived exosomes promotes bone regeneration. *ACS Appl Mater Interfaces*. 2018;10(6):5240–5254.
29. **Narayanan R**, **Huang C-C**, **Ravindran S**. Hijacking the cellular mail: exosome mediated differentiation of mesenchymal stem cells. *Stem Cells Int*. 2016;2016:1–11.
30. **Théry C**, **Amigorena S**, **Raposo G**, **Clayton A**. Isolation and characterization of exosomes from cell culture supernatants and biological fluids. *Current Protocols in Cell Biology*. 2006;30(1):3.22.1–3.22.3.
31. **Théry C**, **Witwer KW**, **Aikawa E**, **et al**. Minimal information for studies of extracellular vesicles 2018 (MISEV2018): a position statement of the International Society for Extracellular Vesicles and update of the MISEV2014 guidelines. *J Extracell Vesicles*. 2018;7(1):1535750.
32. **Webber J**, **Clayton A**. How pure are your vesicles? *J Extracell Vesicles*. 2013;2(1):19861–19866.
33. **Rood IM**, **Deegens JKJ**, **Merchant ML**, **et al**. Comparison of three methods for isolation of urinary microvesicles to identify biomarkers of nephrotic syndrome. *Kidney Int*. 2010;78(8):810–816.
34. **Skwarcz S**, **Bryzek I**, **Gregosiewicz A**, **et al**. Autologous activated platelet-rich plasma (PRP) in bone tissue healing - does it work? Assessment of PRP effect on bone defect healing in animal models. *Pol J Vet Sci*. 2019;22(1):109–115.
35. **Boraldi F**, **Burns JS**, **Bartolomeo A**, **Dominici M**, **Quaglino D**. Mineralization by mesenchymal stromal cells is variously modulated depending on commercial platelet lysate preparations. *Cytotherapy*. 2018;20(3):335–342.
36. **Loebel C**, **Czekanska EM**, **Bruderer M**, **et al**. In vitro osteogenic potential of human mesenchymal stem cells is predicted by *Runx2/Sox9* ratio. *Tissue Eng Part A*. 2015;21(1-2):115–123.
37. **Tu Q**, **Valverde P**, **Chen J**. Osterix enhances proliferation and osteogenic potential of bone marrow stromal cells. *Biochem Biophys Res Commun*. 2006;341(4):1257–1265.
38. **Stein GS**, **Lian JB**, **Stein JL**, **Van Wijnen AJ**, **Montecino M**. Transcriptional control of osteoblast growth and differentiation. *Physiol Rev*. 1996;76(2):593–629.
39. **McKee MD**, **Nanci A**. Osteopontin and the bone remodeling sequence. Colloidal-gold immunocytochemistry of an interfacial extracellular matrix protein. *Ann N Y Acad Sci*. 1995;760:177–189.
40. **Takov K**, **Yellon DM**, **Davidson SM**. Comparison of small extracellular vesicles isolated from plasma by ultracentrifugation or size-exclusion chromatography: yield, purity and functional potential. *J Extracell Vesicles*. 2019;8(1):1560809.
41. **Mol EA**, **Goumans M-J**, **Doevendans PA**, **Sluijter JPG**, **Vader P**. Higher functionality of extracellular vesicles isolated using size-exclusion chromatography compared to ultracentrifugation. *Nanomedicine*. 2017;13(6):2061–2065.
42. **Forteza-Genestra MA**, **Antich-Rosselló M**, **Calvo J**, **et al**. Purity determines the effect of extracellular vesicles derived from mesenchymal stromal cells. *Cells*. 2020;9(2):422.
43. **Benedikter BJ**, **Bouwman FG**, **Vajen T**, **et al**. Ultrafiltration combined with size exclusion chromatography efficiently isolates extracellular vesicles from cell culture media for compositional and functional studies. *Sci Rep*. 2017;7(1):1–13.
44. **Burnouf T**, **Strunk D**, **Koh MBC**, **Schallmoser K**. Human platelet lysate: replacing fetal bovine serum as a gold standard for human cell propagation? *Biomaterials*. 2016;76:371–387.
45. **Tancharoen W**, **Aungsuchawan S**, **Pothacharoen P**, **et al**. Human platelet lysate as an alternative to fetal bovine serum for culture and endothelial differentiation of human amniotic fluid mesenchymal stem cells. *Mol Med Rep*. 2019;19(6):5123–5132.
46. **Valadi H**, **Ekström K**, **Bossios A**, **et al**. Exosome-mediated transfer of mRNAs and microRNAs is a novel mechanism of genetic exchange between cells. *Nat Cell Biol*. 2007;9(6):654–659.

Author information:
- M. Antich-Rosselló, BSc, PhD Student
- M. A. Forteza-Genestra, BSc, PhD Student
  Cell Therapy and Tissue Engineering Group, Research Institute on Health Sciences (IUNICS), University of the Balearic Islands, Palma, Spain; Health Research Institute of the Balearic Islands (IdISBa), Palma, Spain.
- J. Calvo, MD, PhD, Transplant Coordinator
- A. Gayà, MD, PhD, Director
  Cell Therapy and Tissue Engineering Group, Research Institute on Health Sciences (IUNICS), University of the Balearic Islands, Palma, Spain; Health Research Institute of the Balearic Islands (IdISBa), Palma, Spain; Fundació Banc de Sang i Teixits de les Illes Balears (FBSTIB), Palma, Spain.
- M. Monjo, PhD, Senior Lecturer, Principal Investigator
- J. M. Ramis, PhD, Lecturer, Principal Investigator
  Cell Therapy and Tissue Engineering Group, Research Institute on Health Sciences (IUNICS), University of the Balearic Islands, Palma, Spain; Health Research Institute of the Balearic Islands (IdISBa), Palma, Spain; Departament de Biologia Fonamental i Ciències de la Salut, University of the Balearic Islands, Palma, Spain.

Author contributions:
- M. Antich-Rosselló: Contributed to the study conception and design, Acquired and analyzed the data, Contributed to the interpretation of the results, Wrote and re-viewed the main manuscript.
- M. A. Forteza-Genestra: Contributed to the study conception and design, Acquired and analyzed the data, Contributed to the interpretation of the results, Reviewed the manuscript.
- J. Calvo: Provided the hUC-MSCs and PL, Reviewed the manuscript.
- A. Gayà: Provided the hUC-MSCs and PL, Reviewed the manuscript.
- M. Monjo: Contributed to the study conception and design, Contributed to the interpretation of the results, Reviewed the manuscript.
- J. M. Ramis: Contributed to the study conception and design, Contributed to the interpretation of the results, Reviewed the manuscript.

- M. Antich-Rosselló and MA. Forteza-Genestra contributed equally to this work.

Funding statement:
- This research was funded by Instituto de Salud Carlos III, co-funded by the ESF European Social Fund and the ERDF European Regional Development Fund (MS16/00124; PI17/01605), Ministerio de Economía y Competividad (IEDI-2017-00941), and the Direcció General d'Investigació, Conselleria d'Investigació, Govern Balear (grant number FPI/2046/2017) and the Institut d'Investigació Sanitària de les Illes Balears (ITS2018-002-TALENT PLUS JUNIOR PROGRAM, JUNIOR18/01). No benefits in any form have been received or will be received from a commercial party related directly or indirectly to the subject of this article.

ICMJE COI statement:
- None declared.

Acknowledgements:
- The authors thank the Serveis Cientificotècnics of the University of the Balearic Islands (SCT-UIB) for access to their facilities.